Available online at www.sciencedirect.com
SCIENCE DIRECT
Bioorganic & Medicinal Chemistry Letters
Bioorganic & Medicinal Chemistry Letters 16 (2006) 3175–3179

Kinesin spindle protein (KSP) inhibitors. Part 4:[1] Structure-based design of 5-alkylamino-3,5-diaryl-4,5-dihydropyrazoles as potent, water-soluble inhibitors of the mitotic kinesin KSP

Christopher D. Cox,[a,*] Maricel Torrent,[b] Michael J. Breslin,[a] Brenda J. Mariano,[a] David B. Whitman,[a] Paul J. Coleman,[a] Carolyn A. Buser,[c] Eileen S. Walsh,[c] Kelly Hamilton,[c] Michael D. Schaber,[c] Robert B. Lobell,[c] Weikang Tao,[c] Vicki J. South,[c] Nancy E. Kohl,[c] Youwei Yan,[d] Lawrence C. Kuo,[d] Thomayant Prueksaritanont,[e] Donald E. Slaughter,[e] Chunze Li,[e] Elizabeth Mahan,[e] Bing Lu[e] and George D. Hartman[a]

[a]*Department of Medicinal Chemistry, Merck Research Laboratories, PO Box 4, Sumneytown Pike, West Point, PA 19486, USA*
[b]*Department of Molecular Systems, Merck Research Laboratories, PO Box 4, Sumneytown Pike, West Point, PA 19486, USA*
[c]*Department of Cancer Research, Merck Research Laboratories, PO Box 4, Sumneytown Pike, West Point, PA 19486, USA*
[d]*Department of Structural Biology, Merck Research Laboratories, PO Box 4, Sumneytown Pike, West Point, PA 19486, USA*
[e]*Department of Drug Metabolism, Merck Research Laboratories, PO Box 4, Sumneytown Pike, West Point, PA 19486, USA*

Received 15 February 2006; revised 15 March 2006; accepted 16 March 2006
Available online 5 April 2006

Abstract—Molecular modeling in combination with X-ray crystallographic information was employed to identify a region of the kinesin spindle protein (KSP) binding site not fully utilized by our first generation inhibitors. We discovered that by appending a propylamine substituent at the C5 carbon of a dihydropyrazole core, we could effectively fill this unoccupied region of space and engage in a hydrogen-bonding interaction with the enzyme backbone. This change led to a second generation compound with increased potency, a 400-fold enhancement in aqueous solubility at pH 4, and improved dog pharmacokinetics relative to the first generation compound.

Kinesin spindle protein (KSP) has recently been identified as a target for a new generation of antimitotic chemotherapeutic agents that do not interact directly with tubulin.[2] As a member of the kinesin superfamily of molecular motors, KSP (or *Hs* Eg5) couples the energy generated by the hydrolysis of ATP to the production of a motile force that properly organizes the bipolar mitotic spindle during mitosis.[3] Inhibition of KSP results in a mitotic block that leads to apoptosis both in vitro and in vivo,[4] and clinical trials have recently been initiated to determine the potential of a KSP inhibitor (KSPi) to treat cancer in humans.[5]

We recently disclosed 3,5-diaryl-4,5-dihydropyrazole **1** (Fig. 1) as a potent, selective inhibitor of KSP that is active in cells at low nanomolar concentrations;[1a] however, a key impediment to the development of **1** is very poor solubility that prohibits simple aqueous formulation for iv administration. We describe herein an effort to increase potency and water solubility in the dihydropyrazole series that was guided by analysis

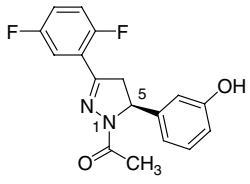

1 KSP IC_{50} = 25 nM

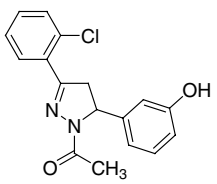

2 KSP IC_{50} = 450 nM

Figure 1. Recently disclosed 3,5-diaryl-4,5-dihydropyrazole inhibitors of KSP.

Keywords: Kinesin spindle protein; Anti-mitotic agents; Structure-based design; Dihydropyrazole.
* Corresponding author. Tel.: +1 215 652 2411; fax: +1 215 652 7310; e-mail: chris_cox@merck.com

0960-894X/$ - see front matter © 2006 Elsevier Ltd. All rights reserved.
doi:10.1016/j.bmcl.2006.03.040

of a computer-generated structural model of an inhibitor–KSP complex. This endeavor led to the installation of an alkylamino side chain at C5 of the dihydropyrazole core to provide a leading compound with increased potency, a 400-fold enhancement in aqueous solubility at pH 4, and improved dog pharmacokinetics relative to **1**.

Target design and chemistry. Although KSPi **1** is a potent, low molecular weight, and synthetically accessible compound, it has water solubility at pH 6.5 of only 29 μg/mL. From the outset of our studies we sought to develop a KSPi suitable for iv administration in an aqueous vehicle; however, simple modifications made in an effort to improve aqueous solubility, including installation of polar functionality in the vicinity of either aryl ring or directly off the N1 position, led to detrimental effects on potency. As a result, we required a new strategy to install solubilizing groups in this series.

Our group recently disclosed the first X-ray crystal structure of a small molecule inhibitor bound to a KSP motor domain construct.[6] Since structural information of the KSP binding site was available to us, we initiated an effort to leverage molecular modeling in combination with available X-ray data to provide guidance for future target selection. To this end, computer-generated molecular models of dihydropyrazole **2** docked into the allosteric site of KSP were produced and analyzed.[7] Our analysis took note of the importance of hydrophobic interactions in the vicinity of both aryl groups, as well as the key location of the N1 acyl group in a solvent exposed area of the binding site (Fig. 2a). Importantly, we also identified unoccupied space above the plane of the dihydropyrazole ring lined with regions of high electron density due to the amide backbone of the enzyme (Fig. 2b).

We hypothesized that substitution of the dihydropyrazole core at C5 could effectively fill the unutilized space and, with optimal placement of functionality, interact favorably with the adjacent polar region pictured in Figure 2b. In this manner, we hoped to enhance both potency and water solubility; however, facile synthetic access to such analogs was not precedented, so we first sought the development of new methodology.

We disclosed in a recent Communication a short and efficient route to exploring SAR in this series (Scheme 1).[8] Beginning with a readily available Weinreb amide (**3**), addition of alkynyl lithiums proceeds cleanly to furnish the propargylic ketones **4**. Conjugate addition by lithium diphenylcuprate occurs readily at −78 °C to furnish β-alkylchalcones **5**. The chalcones are subsequently treated with hydrazine hydrate to form dihydropyrazoles **6** which upon treatment with various electrophiles provide dihydropyrazole ureas **7** in good overall yield.[9] This practical methodology allowed us to quickly investigate the SAR of C5 alkyl substitution.

In vitro SAR and structural analysis. Dihydropyrazole **8a** (Table 1) was chosen as a benchmark compound for the purpose of investigating the effect of C5 substitution on potency.[10] A 10-fold boost in KSP inhibitory activity[11] was immediately realized by installing a methyl substituent at the C5 position of the core (**8b**). We rationalized this result, in part, on the basis of a beneficial interaction from the methyl group with the adjacent hydrophobic area partially filled by the C5 aryl group (Fig. 2a). Addi-

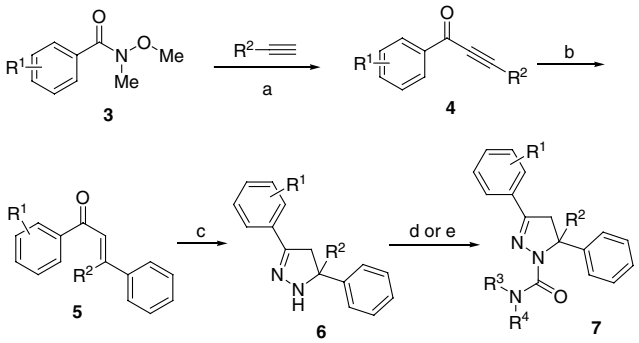

Scheme 1. Reagents and conditions: (a) *n*BuLi, THF, −78 °C to rt; (b) PhLi, CuBr·DMS, THF, −78 °C; (c) $NH_2NH_2{\cdot}H_2O$, EtOH, 150 °C, μ-wave; (d) R^3NCO, CH_2Cl_2; (e) triphosgene, TEA, THF, 0 °C; then R^3R^4NH, TEA.

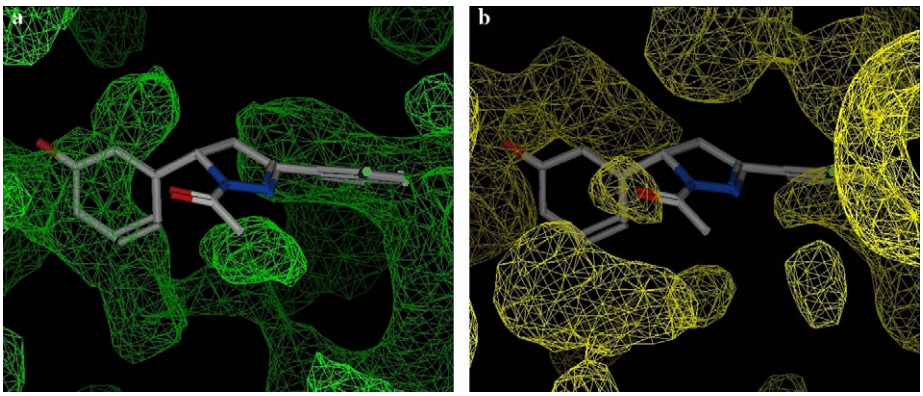

Figure 2. Molecular modeling of KSPi **2** in the allosteric site of KSP. (a) Shown in green are computer-generated hydrophobic regions of the binding site; the aryl rings are predicted to be buried in lipophilic areas of the protein. (b) Shown in yellow are computer-generated polar regions of the binding site; the phenolic OH and carbonyl oxygen are predicted to be residing in polar regions. Notice the unoccupied polar region directly above dihydropyrazole ring.

Table 1. SAR of C5 alkylgroups in 5-alkyl-3,5-diaryl-4,5-dihydropyrazoles

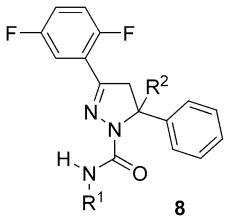

8

Compound	R^1	R^2	KSP IC_{50} (nM)
8a	CH_3	H	3140
8b	CH_3	CH_3	284
8c	CH_3	$(CH_2)_1OH$	903
8d	CH_2CH_3	$(CH_2)_2OH$	606
8e	CH_2CH_3	$(CH_2)_3OH$	745
8f	CH_2CH_3	$(CH_2)_4OH$	697
8g	CH_2CH_3	$(CH_2)_2NH_2$	390
8h	CH_2CH_3	$(CH_2)_3NH_2$	44
8i	CH_2CH_3	$(CH_2)_4NH_2$	67

All values reported are an average for $n = 3$ or greater. The standard deviation limits are within 25–50% of the reported values.

tionally, modeling indicates that the C5 substituent may force the molecule into a lower plane inside the binding pocket (compared to the unsubstituted counterpart **8a**), further burying the aryl rings in the hydrophobic patches located on each side of the cavity.

Continuing our investigation into the SAR of C5 substitution, we found that enhanced polarity in the form of a hydroxymethyl substituent was slightly detrimental to potency as evidenced by **8c**. Likewise, all compounds investigated that had an alkyl group of 2–4 carbons terminated with a hydroxyl substituent (**8d–f**) were less potent than methyl analog **8b**. Replacement of the hydroxyl group with a primary amino group, however, proved more beneficial. Whereas the ethyl linker in **8g** was not optimal, the propyl or butyl linkers in **8h**,**i** provided a more favorable interaction with the amide backbone of the enzyme.

Comparison of the X-ray crystal structures of **2** and **8h** (Fig. 3) in the allosteric site of KSP supported our structure-based design hypothesis.[12] Whereas both inhibitors occupy the same binding site and only very minor changes were seen throughout the protein backbone when comparing the two structures, the primary amino group of **8h** forms a hydrogen-bonding interaction with the backbone carbonyl of Gly117 ($d_{N\text{-}O} = 3.3$Å) that may account for a portion of the observed boost in potency. Of note is the fact that the carbonyl group in **8h** has rotated relative to the carbonyl group in **2** (compare Figs. 3a vs b), the former confirmation being that predicted by molecular modeling. Based on the computer-predicted binding mode of **2**, there appears to be additional hydrophobic space (green area in the foreground of Fig. 2a) that may be reached by alkyl substituents with greater distance from the core, as is the case with the urea linkage in **8h**. This additional hydrophobic interaction may also contribute to an increase in potency within this series.

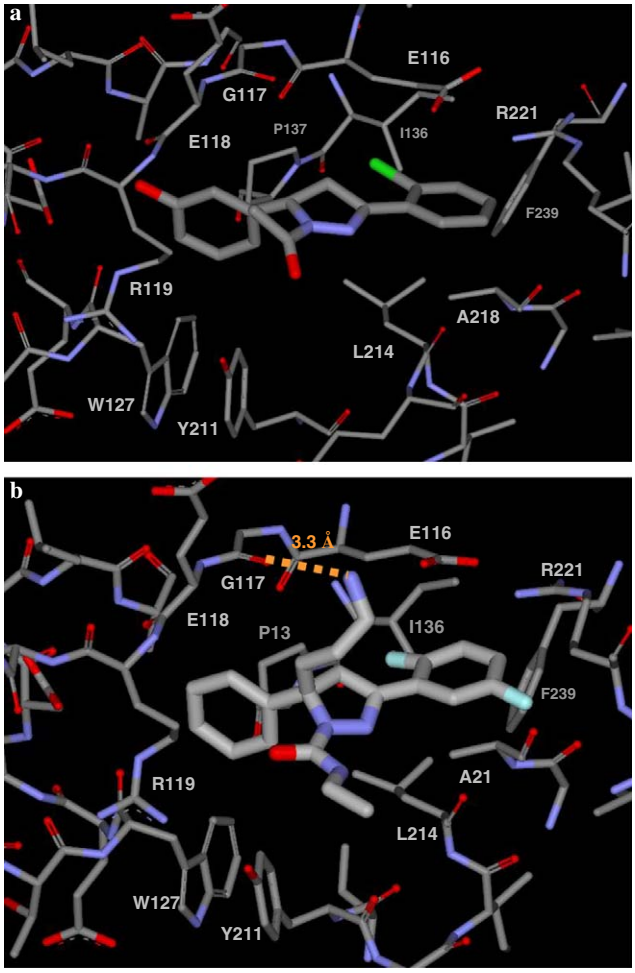

Figure 3. (a) X-ray structure of the allosteric binding site in the KSP-**2**-ADP ternary structure; (b) X-ray structure of **8h** in the binding site.

We next investigated the effects of altering the steric and electronic properties of the butylamino group of **8i** (Table 2). Addition of one (**9a**) or two (**9b**) alkyl groups to form a secondary or tertiary amine reduced potency only slightly relative to the parent; in fact, even the large bicyclic amino group in **9c** was well tolerated. These results are readily explained by the proximity of the key G117 residue to an open, solvent-exposed region of the enzyme that can easily tolerate increased steric bulk. However, reducing the basicity of the amine by tying up the lone pair of electrons in the form of either an *N*-oxide (**9d**) or an amide (**9e**) eliminated the potency enhancement gained from the amino substituent. Attempts to restore the potency seen in the parent molecule by installing moderately basic amines in heterocyclic amides (**9f–h**) were unsuccessful. These results support our hypothesis that a portion of the potency enhancement gained from the C5 alkylamine results from the basicity of the amine, and its ability to form a critical hydrogen bonding interaction.

The SAR in Tables 1 and 2 indicates that a propyl linker with a primary amino functionality (cf. **8h**) offers an optimal potency enhancement for compounds in the C5 alkyl dihydropyrazole series. In an additional

Table 2. SAR of steric and electronic alterations of the primary amino group in 5-butylamino-3,5-diaryl-4,5-dihydropyrazoles

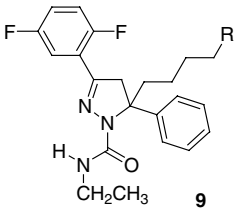

9

Compound	R	ATPase (nM)
9a	–NHBn	100
9b	$-NMe_2$	103
9c		119
9d	$-NMe_2O$	585
9e	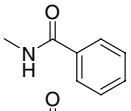	892
9f	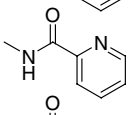	391
9g	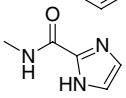	552
9h	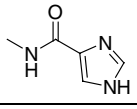	686

All values reported are an average for $n = 3$ or greater. The standard deviation limits are within 25–50% of the reported values.

attempt to improve potency, we probed the SAR of the urea group at N1 as pictured in Table 3. Optimization of the monoethylurea **8h** to the dimethylurea **10a** provided a five-fold boost in potency. Cyclization at the ureido site to form a 4-, 5-, or 6-membered ring (**10b–d**) resulted in modest losses of potency, while the morpholine analog **10e** was even less potent. However, the moderate sensitivity to the nature of the substituent at N1 further supports the notion that this region sits in the solvent-exposed pocket indicated by the computer-generated models and later confirmed by X-ray crystallography. The location and limited size of the hydrophobic pocket identified in the foreground of the active site (Fig. 2a) appear to dictate the binding affinity of these ureido derivatives. In an independent but related series of KSP inhibitors, such a hydrophobic subpocket in the proximity of a polar solvent-exposed area was responsible for making one of two possible stereochemical configurations significantly more potent than its counterpart.[1b]

KSPi **10a** was selected as an optimal compound for further characterization, and its (*S*)-enantiomer, **12**, was

Table 3. SAR of N1 ureas in 5-propylamino-3,5-diaryl-4,5-dihydropyrazoles

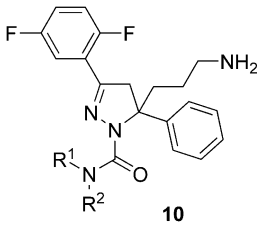

10

Compound	R^1	R^2	ATPase (nM)
10a	CH_3	CH_3	8
10b	$-(CH_2)_3-$		55
10c	$-(CH_2)_4-$		26
10d	$-(CH_2)_5-$		85
10e	$-(CH_2)_2O(CH_2)_2-$		122

All values reported are an average for $n = 3$ or greater. The standard deviation limits are within 25–50% of the reported values.

synthesized as described in Scheme 2.[13] Table 4 directly compares the key properties of **12** with our starting point, compound **1**. Propylamine substitution resulted in a significant increase in potency, both against the isolated enzyme and in cells, and reduced log *P* from 3.1 to 1.2. As predicted, aqueous solubility was dramatically enhanced from 29 μg/mL in **1** at pH 6.5 to greater than 12 mg/mL at pH 4 for **12**. Compound **12** also has improved dog pharmacokinetics relative to **1**, as evidenced by a reduction in clearance and a significant increase in

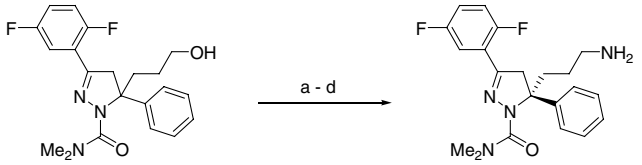

11 **12**

Scheme 2. Reagents and conditions: (a) Chiralpak AD; (b) MsCl, TEA, CH_2Cl_2; (c) NaN_3, DMF, 50 °C; (d) H_2, Pd/C, EtOAc/EtOH.

Table 4. Direct comparison of the properties of **1** and **12**

Property	**1**	**12**
KSP IC_{50} (nM)	24.7 ± 7.5	1.9 ± 1.2
Cell potency[a] (nM)	24.8 ± 4.2	5.2 ± 0.3
log *P*	3.1	1.2
Solubility[b] (mg/mL)	0.029	>12
Dog PK:[c]		
Clearance (mL/min/kg)	22.1 ± 2.3	14.5 ± 7.6
$T_{1/2}$ (h)	1.0 ± 0.1	14.7 ± 7.3
Vdss (L/kg)	1.6 ± 0.4	14.0 ± 0.7
hERG IC_{50}[d] (μM)	26.4 ± 8.1	19.3 ± 0.7

[a] See Ref. 1b for details of this assay.
[b] Both **1** and **12** were crystalline; solubility was determined for **1** in pH 6.5 citrate; for **12**, pH 4.0, citrate was used. The solubility of **12** in water (final pH 10.3) was 1.7 mg/mL.
[c] The compounds were dosed at 0.25 mpk iv to two mongrel dogs, one of each sex.
[d] Values are the average of at least two independent determinations, see Ref. 14 for details of this assay.

half-life. Finally, unlike in a related series of inhibitors where the introduction of a basic amine resulted in greater binding affinity for the potassium channel hERG (human *Ether-a-go-go* Related Gene),[1b,c] the hERG binding of **12** is not significantly increased with respect to **1**.[14]

In conclusion, we have described how the introduction of an alkylamino group at the C5 position of the 3,5-diaryl-4,5-dihydropyrazole core provided access to a series of KSP inhibitors that displayed improved potency, pharmacokinetics, and water solubility relative to the first generation compounds. Of special note is how molecular modeling and X-ray crystallography were employed to identify an unoccupied region of space in the binding site that is effectively utilized in the second generation compounds described herein.

Acknowledgments

We thank Dr. David Dubost for determining the solubility of **12**, Dr. Chuck Ross and Ms. Joan Murphy for high resolution mass spectral analyses, and Drs. Robert Garbaccio and Mark Fraley for helpful discussions and careful reading of the manuscript.

References and notes

1. For the previous papers in this series, see: Part 1: (a) Cox, C. D.; Breslin, M. J.; Mariano, B. J.; Coleman, P. J.; Buser, C. A.; Walsh, E. S.; Hamilton, K.; Huber, H. E.; Kohl, N. E.; Torrent, M.; Yan, Y.; Kuo, L. C.; Hartman, G. D. *Bioorg. Med. Chem. Lett.* **2005**, *15*, 2041; Part 2: (b) Fraley, M. E.; Garbaccio, R. M.; Arrington, K. L.; Hoffman, W. F.; Tasber, E. S.; Coleman, P. J.; Buser, C. A.; Walsh, E. S.; Hamilton, K.; Schaber, M. D.; Lobell, R. B.; Tao, W.; South, V. J.; Yan, Y.; Kuo, L. C.; Prueksaritanont, T.; Shu, C.; Torrent, M.; Heimbrook, D. C.; Kohl, N. E.; Huber, H. E.; Hartman, G. D. *Bioorg. Med. Chem. Lett.* **2006**, *16*, 1775; Part 3: (c) Garbaccio, R. M.; Fraley, M. E.; Tasber, E. S.; Olson, C. M.; Hoffman, W. F.; Torrent, M.; Buser, C. A.; Walsh, E. S.; Hamilton, K.; Schaber, M. D.; Lobell, R. B.; Tao, W.; South, V. J.; Yan, Y.; Kuo, L. C.; Prueksaritanont, T.; Slaughter, D. E.; Shu, C.; Heimbrook, D. C.; Kohl, N. E.; Huber, H. E.; Hartman, G. D. *Bioorg. Med. Chem. Lett.* **2006**, *16*, 1780.
2. Wood, K. W.; Cornwell, W. D.; Jackson, J. R. *Curr. Opin. Pharmacol.* **2001**, 370.
3. (a) Heald, R. *Cell* **2000**, *102*, 399; (b) Sharp, D. J.; Rogers, G. C.; Scholey, J. M. *Nature* **2000**, *407*, 41; (c) Mandelkow, E.; Mandelkow, E.-M. *Trends Cell Biol.* **2002**, *12*, 585; (d) Endow, S. A.; Barker, D. S. *Annu. Rev. Physiol.* **2003**, *65*, 161.
4. (a) Mayer, T. U.; Kapoor, T. M.; Haggarty, S. J.; King, R. W.; Schreiber, S. L.; Mitchison, T. J. *Science* **1999**, *286*, 971; (b) Sakowicz, R.; Finer, J. T.; Beraud, C.; Crompton, A.; Lewis, E.; Fritsch, A.; Lee, Y.; Mak, J.; Moody, R.; Turincio, R.; Chabala, J. C.; Gonzales, P.; Roth, S.; Weitman, S.; Wood, K. W. *Cancer Res.* **2004**, *64*, 3276.
5. (a) Coleman, P. J.; Fraley, M. E. *Expert Opin. Ther. Patents* **2004**, *14*, 1659; (b) Duhl, D. M.; Renhowe, P. A. *Curr. Opin. Drug Discov. Dev.* **2005**, *8*, 431.
6. Yan, Y.; Sardana, V.; Xu, B.; Homnick, C.; Halczenko, W.; Buser, C. A.; Schaber, M.; Hartman, G. D.; Huber, H. E.; Kuo, L. C. *J. Mol. Biol.* **2004**, *335*, 547.
7. In our recently disclosed structure, the KSPi occupies an 'induced fit' pocket 12 Å from the nucleotide binding site. This pocket, not present in the apo structure of KSP, has been termed the allosteric site. Compound **2** was chosen for docking because it was the first sub-micromolar lead compound we discovered in this series, and these studies were initiated before **1** was fully characterized. Additionally, the in silico predicted pose of **2** was later confirmed by X-ray crystallography (Fig. 3a), affording more confidence to the predictions made from our modeling efforts.
8. Cox, C. D.; Breslin, M. J.; Mariano, B. J. *Tetrahedron Lett.* **2004**, *45*, 1489.
9. Intermediate **6** could also be treated with acyl chlorides to provide the analogous dihydropyrazole amides (see Ref. 8); however, for the purposes of this Communication, we will focus only on dihydropyrazole ureas **7**.
10. The phenol functionality on the 'eastern' phenyl group of **1** and **2** is not present in subsequent analogs because we generally see only a modest increase (<10-fold) in potency due to its presence (Ref. 1c), and also because of the known drawbacks of phenol-containing drugs, namely propensity for electrophilic activation; see: Zhou, S.; Chan, E.; Duan, W.; Huang, M.; Chen, Y.-Z. *Drug Metab. Rev.* **2005**, *37*, 41.
11. KSP inhibitory activity was measured using a standard ATPase assay; see: Breslin, M. J.; Coleman, P. J.; Cox, C. D.; Culberson, C. J.; Hartman, G. D.; Mariano, B. J.; Torrent, M. PCT WO 079973 A2, 2003.
12. The experimental data for the KSP-**2**-ADP structure have been reported previously (Ref. 1a). KSP-**8h**-ADP structure: co-crystals of the ternary complex of KSP-ADP(Mg^{2+})-monastrol were first formed with the vapor diffusion method (see Ref. 6). The KSP monastrol ternary crystals then soaked in the harvest solution (28% PEG3350, 0.2 M K_2HPO_4 at pH 8.0) containing 2 mM **8h** for 3 days to replace monastrol at the inhibitor binding site. The X-ray diffraction data were collected at 100 K to 2.51 Å resolution in the space group $P2_12_12_1$ with cell dimensions of $a = 68.7$ Å, $b = 79.6$ Å, and $c = 158.7$ Å ($R_{sym} = 0.047$ and completeness = 99%). The ternary complex structure of KSP-**8h**-ADP(Mg^{2+}) was determined by the use of the difference Fourier method and refined to an R-factor of 0.234 ($R_{free} = 0.279$). The coordinates have been deposited with RCSB Protein Data Bank under the accession code 2G1Q.
13. Compound **11** was synthesized by the general procedure described in Ref. 8. Separation of the enatiomers of **11** was carried out on a 5 cm Chiralpak AD column at a flow rate of 80 mL/min with an eluent of 15% 2-propanol in hexanes containing 0.1% diethylamine as a modifier. Under these conditions, the first enantiomer to elute was more potent in the ATPase assay (190 vs. 8200 nM for the second eluting isomer) and was carried on to provide **12** as described in Scheme 2. The (*S*)-stereochemistry is assigned by analogy to our previous work (Ref. 1a).
14. Blockade of the hERG channel has been implicated in drug-induced prolongation of the QT_c interval of the EEG, an observation that has been linked to potentially fatal ventricular arrhythmias. The hERG IC_{50} values were determined by radioligand competition experiments using membrane preparations from human embryonic kidney cells that stably express hERG. For assay details, see: Bilodeau, M. T. et al. *J. Med. Chem.* **2004**, *47*, 6363, and references therein.